energies

Article

Cost Optimal Renewable Electricity-Based HVAC System: Application of Air to Water or Water to Water Heat Pump

Boris Delač [1], Branimir Pavković [1,*], Marino Grozdek [2] and Luka Bezić [1]

[1] Department of Thermodynamics and Energy Engineering, Faculty of Engineering, University of Rijeka, Vukovarska 58, 51000 Rijeka, Croatia; boris.delac@riteh.hr (B.D.); lbezic@riteh.hr (L.B.)
[2] Department of Applied Thermodynamics, Thermal and Process Engineering, Faculty of Mechanical Engineering and Naval Architecture, University of Zagreb, Ivana Lučića 5, 10000 Zagreb, Croatia; marino.grozdek@fsb.hr
* Correspondence: branimir.pavkovic@riteh.hr

Abstract: This paper aims to determine cost optimality between heating, ventilation and air conditioning (HVAC) systems operating with air to water heat pumps (AWHP) and water to water heat pumps (WWHP). The analysis is performed for a certain number of heat pump units with fixed and variable capacity made by four manufacturers available on European market. Simulations are performed in Trnsys software. The results show that heat pump partial load efficiency should not be neglected in analysis of application while the difference in energy consumption and costs can be up to 17%. The requirement for performing analysis on a wider range of units is indicated, especially when heat pump systems with different sources are considered. HVAC system with AWHP units with capacity control is a cost optimal solution for case study nursery building operating on the Croatian coast. The application of the photovoltaic (PV) array sized to cover nonrenewable part of electricity consumed in HVAC system has a return period of 12 years. It is determined that seasonal efficiency indicators from relevant European database do not support unit operation.

Keywords: heat pump; efficiency; part load; simulation

check for updates

Citation: Delač, B.; Pavković, B.; Grozdek, M.; Bezić, L. Cost Optimal Renewable Electricity-Based HVAC System: Application of Air to Water or Water to Water Heat Pump. *Energies* **2022**, *15*, 1658. https://doi.org/10.3390/en15051658

Academic Editors: Damir Dovic and Vladimir Soldo

Received: 27 January 2022
Accepted: 21 February 2022
Published: 23 February 2022

1. Introduction

Heat pumps represent a promising solution to achieve cost optimal nearly zero energy building (nZEB) [1–6]. Energy efficiency of heat pump strongly depends on heat source temperature (ambient air, ground water, solid soil, or chilled water) and heat sink temperature (e.g., temperature in heating system, domestic hot water (DHW) temperature or cooling water temperature). Operating parameters and efficiency of the heat pump constantly change during the operation and adapt to temperatures of heat source and heat sink, while the control system changes the compressor and unit capacity.

Heat pump performance is strongly affected by the design of the heating or cooling system. During the year, almost all systems operate with 80% to 90% time at a low load that is 50% or less of the maximum load, with the compressor operating with 25% or less of maximum power [7]. Numerous authors have conducted research on the reduction of efficiency caused by an on–off control of heat pumps. Uhlmann and Bertsch [8] concluded that frequent cycling of the unit leads to higher losses compared to continuous operation of the unit. Waddicor et al. [9] determined that the control strategy has the greatest impact on the overall reduction in efficiency due to short device operation. These authors determined minimum device operating time of 15–20 min to avoid the reduction in efficiency. Riviere et al. [10] found that the decrease in efficiency is associated with the set point temperature and a low hysteresis of the control thermostat. The improvement can be achieved by increasing the water accumulation volume in the case of an indirect system. Fahlen [7] discussed the importance of control in the performance of heat pump and states the advantages of modern electric motors of a variable speed with frequency control, which allows less on–off cycling of the device and continuous operating time, reducing frost on the air source units, reduction of differences in temperatures in evaporators and condensers and thus a more favorable thermodynamic process.

Equipment of heating, ventilation and air conditioning (HVAC) system including heat pumps is selected according to maximum thermal load in design conditions. System control and operation at partial loads can have a significant impact on the annual energy consumption of a heat pump. Data on heat pump performance for nominal capacities and different source and sink temperatures are usually presented in manufacturers' catalogues, while data for partial loads are often omitted, even for heat pumps with capacity control.

Relevant certification rules such as [11] establish procedures to estimate seasonal coefficients of performance (SCOP and SEER) for assumed energy consumption profile during the year and assumed climate data. Such seasonal efficiency is not a sufficient indicator for the evaluation of all cases of application as the consumption profile during the operation as total energy differs between cases and thus affects the final efficiency. Besides, the lifetime of the heat pump unit depends on the chosen temperature regime, the quality of heat pump components, and operational settings of the control system as well as on the number of on/off cycles during the operation, and this strongly influences the lifetime costs. Therefore, the case dynamic simulation of every case of heat pump application will give more reliable indicators for economic evaluation. Energy consumption for auxiliary equipment can also have a significant impact on the final efficiency of the system.

An important issue for designers is the choice of the heat source in cases with multiple heat sources availability. Schibuola and Scarpa [12] conducted the measurement and compared the seasonal efficiencies of water to water heat pump (WWHP) and air to water heat pump (AWHP) systems for a facility in Venice, Italy. WWHP achieves a 20 to 30% higher SCOP than the AWHP, but for full consideration it was necessary to include consumption of auxiliary energy of pumps, which are needed for WWHP system operation. Therefore, the SCOP and SEER of the system with WWHP was proven to be 20% lower than for the sole WWHP unit. Zaca et al. [13] considered the example of a residential building in southern Italy and found that the ground source heat pump system represents a cost-effective solution for warm Mediterranean climate with dominant cooling. Marini [14] conducted an analysis on multifamily buildings located in Milan, Rome and Palermo and concluded that the optimal source for heat pump operation in a colder climate is soil, while in warmer climates, air is a more favorable thermal source due to lower investment and operating costs. Filotico et al. [15] compared WWHP with seawater as a source with AWHP through Trnsys simulation. They concluded that the coefficient of performance (COP) of the WWHP unit is uniform throughout the year due to a small change in source temperature and ranges from 4 to 4.5, while one from the AWHP unit varies from 1.4 to 4.4. Operating efficiency and heat capacity of air source heat pumps can be affected by frost formation of the evaporator during the winter months. Wang et al. determined the optimal time point to initiate the defrosting of an air source heat pump [16]. Rossi di Schio et al. [17], in their study of AWHP efficiency in Italy, determined the importance of considering defrosting cycles and the large differences between performance in real weather data compared to their performance in a standard test reference year.

The research presented in this paper will address the problem of selection between AWHP and WWHP technology for the HVAC system with a specific consumption profile. Moreover, it will determine the influence of partial load operation characteristics on the energy use. The method used comprises conducting a preliminary design of the heat pump system and annual dynamic simulation with the aim of revealing real energy consumption and efficiency during operation. Conducting this type of energy simulation requires complete performance data for the whole operating temperature range of the heat pump unit, and the whole range, or a few selected partial load steps, in the temperature operational range for capacity control. The problem of missing input data for such an analysis will be addressed in the paper as well. Heat pump units presented and analyzed in the paper are WWHP and AWHP produced by several different manufacturers present on the European market. Differences between those units addressed in the paper comprise investment costs, efficiencies, capacity control and manufacturers' data, which are necessary to conduct dynamic simulation.

2. Method

2.1. Energy

Energy consumption of compression heat pump system consists of electricity consumption of heat pump unit and auxiliary energy required to operate the system.

$$E_{\mathrm{s}} = E_{\mathrm{hp}} + E_{\mathrm{aux}} \tag{1}$$

During the year compression heat pump operates to produce required heating and cooling energy with electric energy consumption presented in Equation (2).

$$E_{\mathrm{hp}} = E_{\mathrm{hp,h}} + E_{\mathrm{hp,c}} \tag{2}$$

Heat pump electricity consumption is calculated as a function of performance coefficient of heat pump, coefficient of performance (*COP*) for heating and energy efficiency ratio (*EER*) for cooling.

$$E_{\mathrm{hp,h}} = Q_{\mathrm{hp,h}}/COP \tag{3}$$

$$E_{\mathrm{hp,c}} = Q_{\mathrm{hp,c}}/EER \tag{4}$$

Performance coefficient (*COP* and *EER*) primarily depends on heat source and sink temperatures and unit design, but it is also a function of unit efficiency, which differs between full and partial load operation. Coefficient of performance (*COP* or *EER*) at partial load can be estimated using the partial load factor (*PLF*), which is applied to the performance coefficient determined for operation at full capacity.

$$COP = PLF \cdot COP_{100\%} \tag{5}$$

or

$$EER = PLF \cdot EER_{100\%} \tag{6}$$

Several approaches are available to determine heat pump energy consumption during the partial load operation. The calculation methods in standards ASHRAE 116-1995 [18] and EN 14825 [19] are based on a bin method and comprise the seasonal coefficient of performance (*SCOP* or *SEER*). In short, these standards consider the degradation of performance coefficient with a decrease of load ratio in cyclic operation and stand-by energy losses. The problem with the application of this method for dynamic simulations is that the decrease in efficiency is assumed for all cases of partial loads, which is not true for a certain number of new designs of heat pumps in the market. Depending on the heat pump design, the efficiency in the partial load can increase or decrease and that data are not always present in manufacturer's catalogues.

The most widespread approach in analyses which can be found in recent studies is the one which neglects the partial load efficiency change ($PLF = 1$). The approach is frequently used due to incomplete manufacturer's technical data for heat pump units and the lack of a standard for general estimation of efficiency at a partial load. This type of calculation would certainly be unreliable as the efficiency of the unit greatly depends on the design and components of the heat pump unit. Some manufacturers provide performance data for the complete capacity range which ensures the conduction of dynamic simulations with a partial load efficiency. In the case where only some of the manufacturer's data are available (e.g., efficiency at the single reduced capacity stage), the complete range of performance can be obtained using the Italian standard UNI 10963 [20].

The range of WWHP and AWHP units included in this research comprises fixed capacity and variable capacity units. The simulations for the case study below are conducted in two scenarios. In the first scenario (S1), the change in partial load efficiency is neglected

(PLF = 1) for both fixed and variable capacity units of AWHP and WWHP units. In this way there is no advantage in performance given to any of the considered AWHP and WWHP units. The second scenario (S2) comprises simulations with the change in partial load efficiency. It is considered only for variable capacity units with the provided relevant data in the manufacturer's catalogues.

The impact of partial load efficiency can be determined when the ratio of energy consumption in scenario 2 to energy consumption in scenario 1 for the same system is evaluated as:

$$X = E_{\mathrm{s,s2}}/E_{\mathrm{s,s1}} \tag{7}$$

The goal of the heat pump application is not only a cost reduction for the consumer, but also an increase in the renewable energy share in total energy consumption. The following case study analysis is intended to present the system design which enables "renewable energy heating and cooling system". This means that other building electricity consumption besides heating, cooling and heating the consumption water is not included in the consideration and that it is not necessary to consider all criteria for "zero energy building". The only criterion is that entire energy necessary for heating and cooling should be renewable. Non-renewable and renewable energy sources make up the energy consumption structure of the compression heat pump system. Those are ambient heat and electric energy. Electric energy structure by source is different for each country. Using the national share of nonrenewable energy (f_{nren}), which is evaluated using the structure of electric energy use for Croatia [21] and Eurostat data [22], the non-renewable part of consumed electricity linked to carbon dioxide emissions can be estimated at approximately 50% (f_{nren} = 0.5) and can be calculated as:

$$E_{\mathrm{s,nren}} = E_{\mathrm{s}} \cdot f_{\mathrm{nren}} \tag{8}$$

PV system size will be applied to cover the nonrenewable part of consumed electricity.

$$E_{\mathrm{PV}} > E_{\mathrm{s,nren}} \tag{9}$$

The grid electricity consumption with PV system is calculated as follows:

$$E_{\mathrm{s,PV}} = E_{\mathrm{s}} - E_{\mathrm{PV}} \tag{10}$$

Indicator of energy consumption is derived using a net usable building area.

$$EI = E_{s,\mathrm{PV}}/A \tag{11}$$

2.2. Costs

The global cost is considered through investment, operating and maintenance cost. By applying the discount rate by means of a discount factor, global costs are expressed in terms of value in the starting year:

$$C_g(\tau) = C_I + \sum_j \left[\sum_{i=1}^{\tau} \left(C_{a,i}(j) \times R_d(i) \right) - V_{f,\tau}(j) \right] \tag{12}$$

where τ is the calculation period, C_{I} is the initial investment cost for HVAC and PV system, C_{a} is the annual operating cost multiplied by R_{d} which is the average discount factor calculated for each year of the evaluation period, and $V_{\mathrm{f},\tau}$ is the average residual value at the end of the evaluation period and it can be included into calculation if it exists. It is not included in present analysis, as the lifetime of HVAC and PV system is assumed to be equal for the considered period. This calculation procedure is repeated for each year of calculation period. The discount factor is calculated as:

$$R_{\mathrm{d}}(p) = (1/(1 + \mathrm{r}/100))^p \tag{13}$$

where p is the number of years from the starting period and r is the real discount rate.

Indicator of global cost CI is derived using a net usable building area.

$$CI = C_g/A \tag{14}$$

3. Case Study

3.1. Building

The considered building is located on the Adriatic coast in Poreč (Croatia). It is in the protected cultural and historical zone and listed in the Register of Cultural Heritage of the Republic of Croatia. It was built in 1912 as a detached building with U-shaped floor plan and a total usable area of 690 m^2. This three-story building is used as a nursery. The attic is unheated and ventilated. The walls are massive, built from 75 cm thick stone. Carpentry is wooden with a single float glass. The main characteristics of the building are presented in Table 1.

Table 1. Main characteristics of the building regarding physics, operation, and climate data.

Climate data	City	Poreč (Croatia)
	Longitude	17°36′ E
	Latitude	45°13′ N
	Dry bulb temperature-annual daily mean	13.9 °C
	Dry bulb temperature-daily mean minimum	−6.5 °C
	Dry bulb temperature-daily mean maximum	29.6 °C
	Mean relative humidity	74%
	Global irradiation	1428 kWh/m^2
Physics	Dimensions (length × width × height)	24.4 m × 15.5 m × 20.5 m
	Conditioned area	690 m^2
	Conditioned volume	5045 m^3
Envelope	External wall *U*-value	1.4 W/m^{2}K
	Internal wall *U*-value	1.5 W/m^{2}K
	Floor on the ground *U*-value	1.7 W/m^{2}K
	Roof *U*-value	3.1 W/m^{2}K
	Ceiling towards the attic *U*-value	1 W/m^{2}K
	Window/door *U*-value	3.2 W/m^{2}K
Ventilation	Infiltration/required ventilation rate	0.48 h^{-1}/1.32 h^{-1}
	Mechanical ventilation	Not existing
Occupancy and operation	Occupancy	5 days in week 6 A.M.–5 P.M.
	Number of persons	120
	Internal heat gains	6 W/m^2
	Heating and cooling operation	Interrupted
	Heating temperature set point	22 °C
	Cooling temperature set point	24 °C
	DHW set point	45 °C

With the increase in computing capacity, the use of numerical dynamic simulations has become a standard practice to estimate the performance of buildings and HVAC systems. Among the suitable software for performing dynamic simulations, Trnsys [23] software is used due to the author's experience in using this software. The building dimensions and envelope parameters were taken from the architectural project for building envelope refurbishment and was used to build a thermal model. The building is modeled by Trnsys Type 56 multi zone model from the standard model library. According to the requirements for heating and cooling (H/C) of individual rooms, the simulation model is divided into 17 thermal zones. A zone represents the area of specific purpose and usage regimes. In each zone, the air state is homogeneous at any given time step. The approach is proven to be one of the most appropriate tools for analyzing the energy balance of a building and its systems from the point of view of accuracy and consumption of computational time. Figure 1 shows the building photo and the corresponding model created using Google SketchUp with a Trnsys3d plugin.

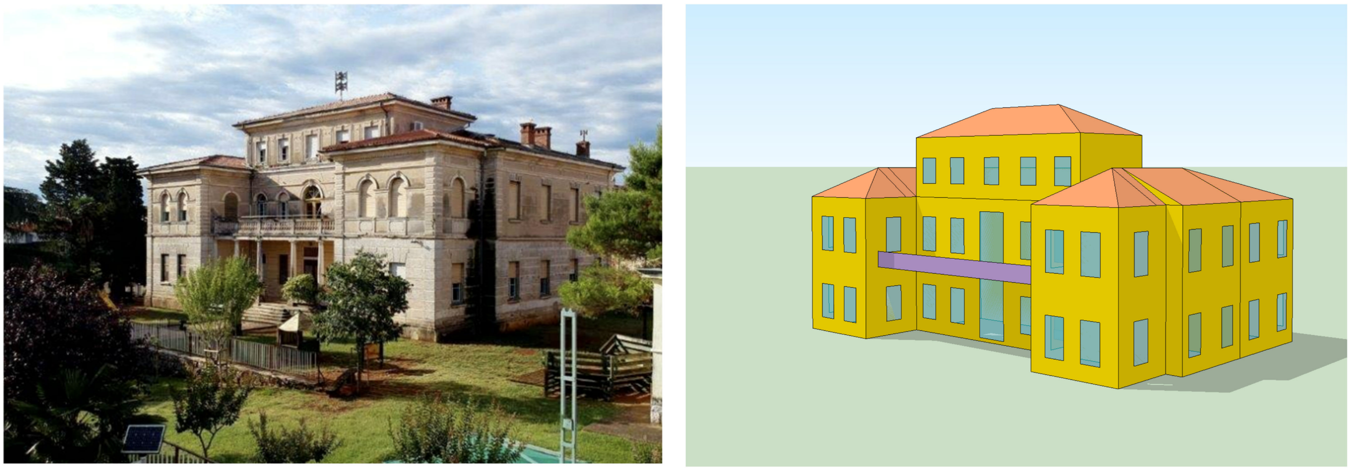

(**a**) (**b**)

Figure 1. (**a**) Case study building; (**b**) the model created using Google Sketchup with Trnsys3d.

Occupancy and operating conditions are acquired from the employed staff. The main model assumptions are described in the following. The nursery is used 5 days a week, from 6 AM to 5 PM, with interruptions in conditioning of spaces outside working hours. Set point temperature is 22 °C for heating period and 24 °C for cooling period. Number of air changes per hour is calculated considering infiltration and the required air change rate for that type of building during operating hours [24].

Although it is not necessary in Croatian rules for analysis in energy certification of educational buildings, the central DHW heating system is considered and DHW consumption is included in the calculations. According to Ref. [25] DHW consumption equals in range from 5 to 15 L/person/day at the temperature of 45 °C. For approximate 250 days of operation during the year, consumption of 10 L/day/person and inlet cold water temperature 13.5 °C the useful energy for DHW heating is 10,990 kWh.

The annual simulations of energy consumption for heating and cooling are performed in meteorological boundary conditions of the synthetic test reference year (TRY), which is created for the location of Poreč using Meteonorm software [26]. This software uses measured data from nearby weather stations and satellite measurement data to create meteorological parameters in a time step of one hour (total solar irradiance, air temperature and relative humidity, wind speed and precipitation). The interpolation of air temperature and wind speed considers additional geographic parameters of the site due to the surrounding area, distance from water surfaces or mountains, nearby structures, and orientation. The influence of the seacoast is accounted for by increased wind speeds in all months, increased temperatures in winter, and lower temperatures in the summer. The created dataset from TRY data for the location Poreč has identical statistical properties as the available monthly minimum, maximum and average values provided by the Croatian Meteorological and

Hydrological Service [27]. Linear interpolation was used to adjust the data from the hourly to the simulation time step.

The annual thermal energy consumption for heating and cooling of the building is determined by a numerical dynamic simulation, which resulted in useful energy for heating the building of 61,007 kWh (88.4 kWh/m^2) and for cooling the building, 31,301 kWh (45.4 kWh/m^2).

The validation of building model is performed by a comparison of the simulation results to the long-term consumption of fuel oil, the procurement of which is monitored in the National energy management information system in the period from 2010 to 2019. Average annual consumption of fuel oil in the monitored period is 9900 L (Figure 2). During the monitoring period, fuel oil was used in standard fuel oil boiler for building heating and central DHW heating. Thermal energy from heating oil is 98,906 kWh (calculated with a lower heating value of 9.69 kWh/L).

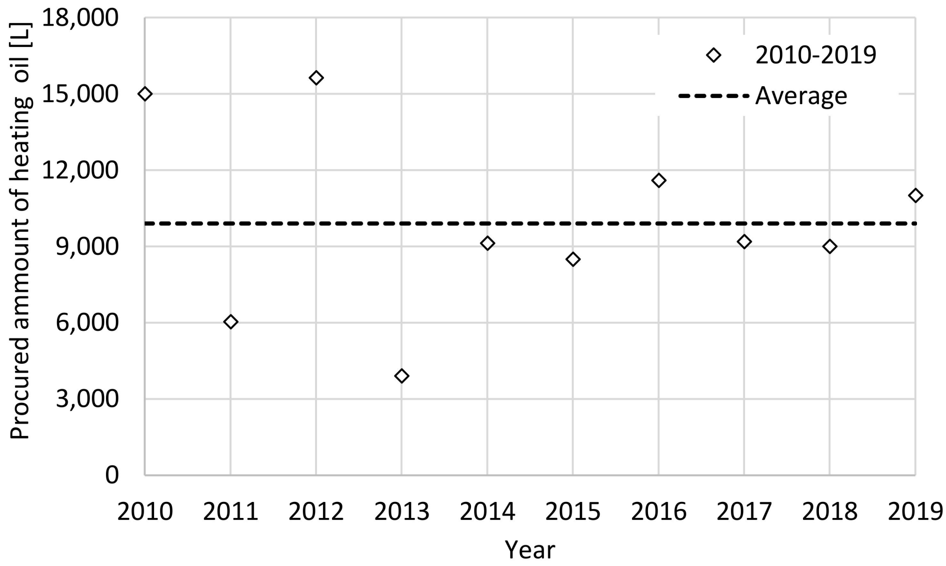

Figure 2. Procurement of heating oil in the period from 2010 to 2019.

The consumption of useful energy for heating and DHW from simulation is 71,997 kWh, which is 73% of the available thermal energy calculated from heating oil consumption. The difference simulated and measured values can be addressed to system losses in production and distribution of thermal energy. The presented calculation has validated the building simulation model and confirmed suitability for further analyses.

Due to heritage status, interventions which affect the appearance of the building are not allowed and only two energy efficiency measures on the building envelope are allowed. Those are thermal insulation of the ceiling towards the unheated attic and the replacement of windows and transparent surfaces. By applying 12 cm thick layer of mineral wool to the outer side of the ceiling towards the attic, the heat transfer coefficient will be reduced to 0.225 W/m^{2}K. The new carpentry will be double-winged with wooden frame and thermal insulated glass (U_w 1.4 W/m^{2}K).

The consumption of thermal energy for heating and cooling the building after implementation of energy efficiency measures (EEM), which results from the simulation shown in Figure 3. The total energy use for heating the building is 53,421 kWh (77.4 kWh/m^2), and the energy for cooling is 31,792 kWh (46.1 kWh/m^2). Design loads for heating and cooling are determined for the building in the state after implementation of energy efficiency measures. Design load for building heating of 85 kW is calculated according to the methodology proposed in EN 12831 [28]. Design load for building cooling of 65 kW is acquired by performing the calculation procedure from VDI 2078 [29]. From Figure 3 it is obvious that partial loads prevail.

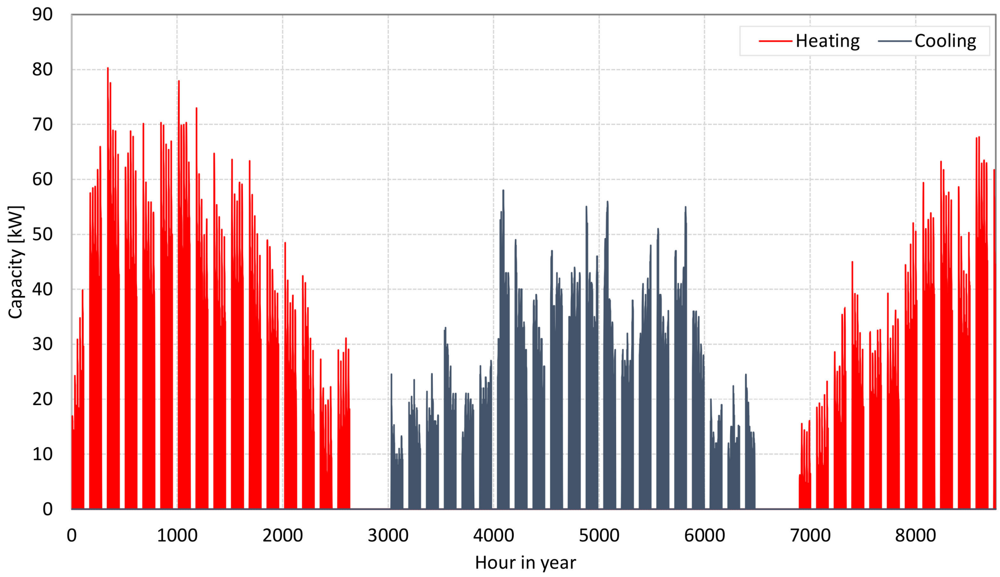

Figure 3. Useful energy for heating and cooling (after implementation of EEM).

3.2. Building Energy Systems

In the state before renovation the building was heated by hot water radiators within the two-pipe hydronic heating system with an oil fueled boiler. Air conditioning of the building was not present at all. The boiler room is located in the auxiliar building situated close to the main building. The reconstruction of the HVAC system includes the complete dismantling of the equipment in the boiler room, existing radiators and the pipe network and the installation of a new heating and cooling system.

Design project of renovation including the heating and cooling system with WWHP was presented to the authors of this paper with the demand to check the feasibility of the proposed energy efficiency measures. The authors performed the case study, considering the AWHP application as well. Based on the results of that study AWHP emerged as a better solution than WWHP considering cost efficiency. In the authors' previous experience [30–32], WWHP systems were usually more feasible than AWHP even for application in mild Mediterranean climate. Driven by the results of the case study for the here-presented building, the authors performed a wider analyses presented in this paper.

Two hydronic systems with heat pumps are considered in the present paper: a ground water source heat pump system and an air source heat pump system.

The equipment for producing heating and cooling energy and DHW is positioned in the existing boiler room. The distribution and transfer of thermal energy within the building is identical for both versions (AWHP and WWHP) of the system: heating and cooling is provided through fan coil units. Only for sanitary spaces are radiators provided. In the heating season, the water temperature is 45/40 °C, while in the cooling season, the water temperature in the system is 7/12 °C.

A storage tank for DHW is selected using the guidelines from Ref. [25] Tank volume is 450 L with coiled tube heat exchanger inside the tank. It is common to anticipate heating the tank from the initial to the operating temperature within 1 h, which in the considered case results in 16.5 kW of heat exchanger capacity. The recirculation losses are considered for a recirculation line loop, which is present in the building and the assumed operation period. An approximate DHW usage pattern is acquired from the representatives of the nursery (Figure 4). DHW is used for the hygienic needs of the users (washing hands) and in the kitchen of the nursery (for preparing meals and washing dishes). According to the daily schedule in the nursery, lunch takes place at 11:30, so a higher consumption of DHW occurs from 12 to 13 h for washing dishes.

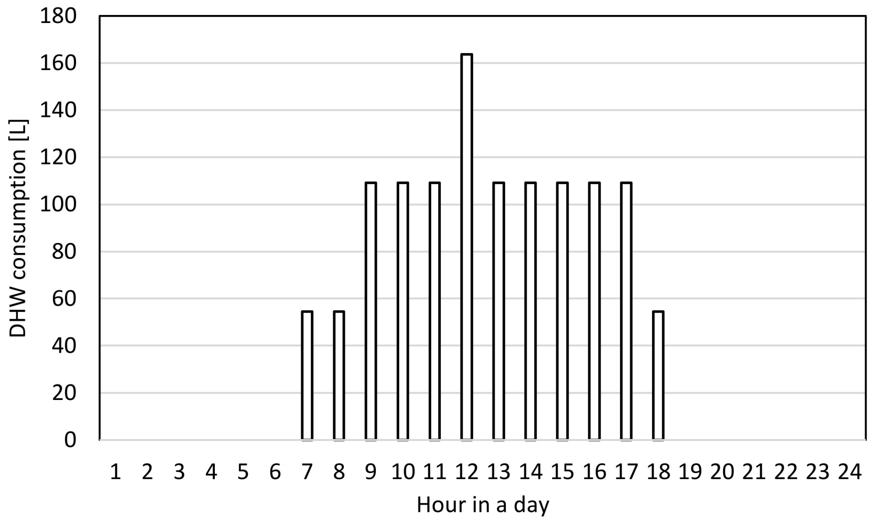

Figure 4. Assumed DHW consumption profile.

Distribution pipelines between the heat production and emission equipment are designed based on the required capacities and temperature differences followed by the procedure from Ref. [25] Pumps are selected from the manufacturer catalogs based on the required volumetric flow rate and the total pressure drop.

In the following, the elements of the heat production subsystems are summarized and presented at the level of the conceptual design, which is necessary to understand the simulations and calculations performed.

3.2.1. HVAC System with WWHP

The system uses a ground water via supply and return wells as a heat source and sink for water-to-water heat pumps. Figure 5 shows the positions of the main buildings and the auxiliary buildings with the HVAC equipment, and the positions of supply (B-1) and return (B-2) wells. Each of the wells is bored to the depth of 30 m with a diameter 300 mm. The building is positioned 110 m from the seashore, 9 m above sea level.

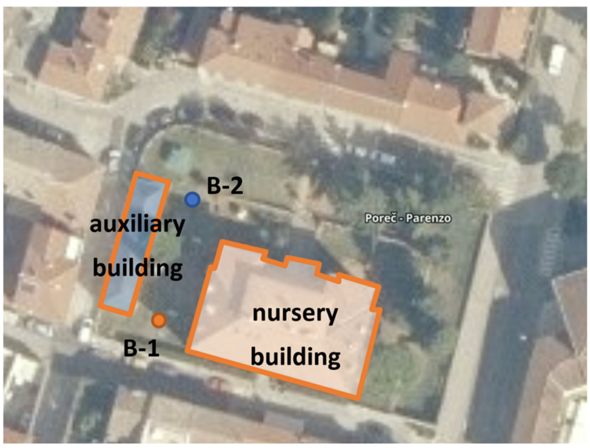

Figure 5. The positions of buildings and wells (B-1 supply well, B-2 return well).

Due to the small distance between the coast and the wells, the sea temperature directly affects the temperature of the pumped water at the wells. Good permeability and porosity of limestone deposits very quickly increases the proportion of seawater compared to fresh or brackish water during the water supply. The assumed pumping takes place at a depth of 10 to 28 m where there is no significant impact on the atmospheric conditions during the year. Given the relatively small volume of water supplied and the volume of porous soil between the seashore and the wells, no significant drop in water temperature is expected during the winter months. Therefore, it is possible to assume a small annual amplitude of water temperature change at the production well. The annual temperature of the well water can be obtained as the arithmetic mean of the sea surface temperature during the year, given the assumption that the mean annual sea temperature is equal to the stationary sea temperature at the specified pumping depth. It turns out that the well temperature will be approximately 17 °C, and it is predicted that its deviation during summer/winter will be up to +/−2 °C (Figure 6).

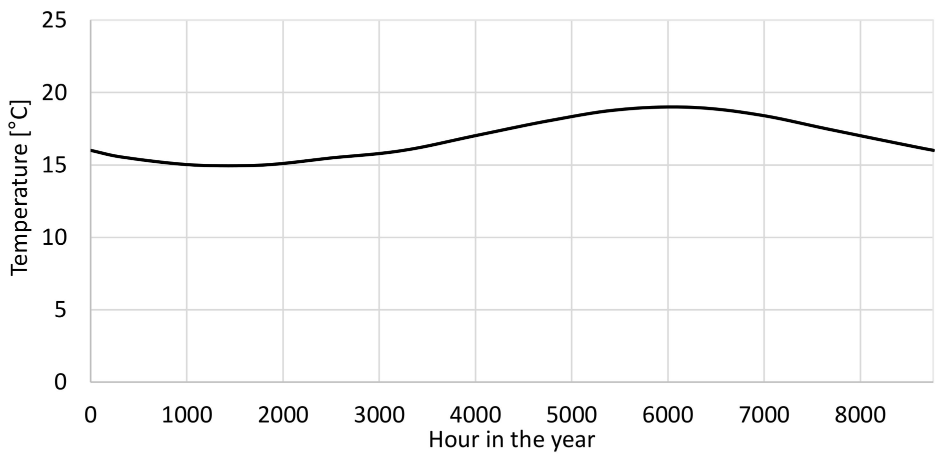

Figure 6. Temperature of groundwater at the supply well.

A simplified schematic representation of the heat production subsystem with wells, pumps, heat exchangers, heat pumps and the necessary control valves is given in Figure 7.

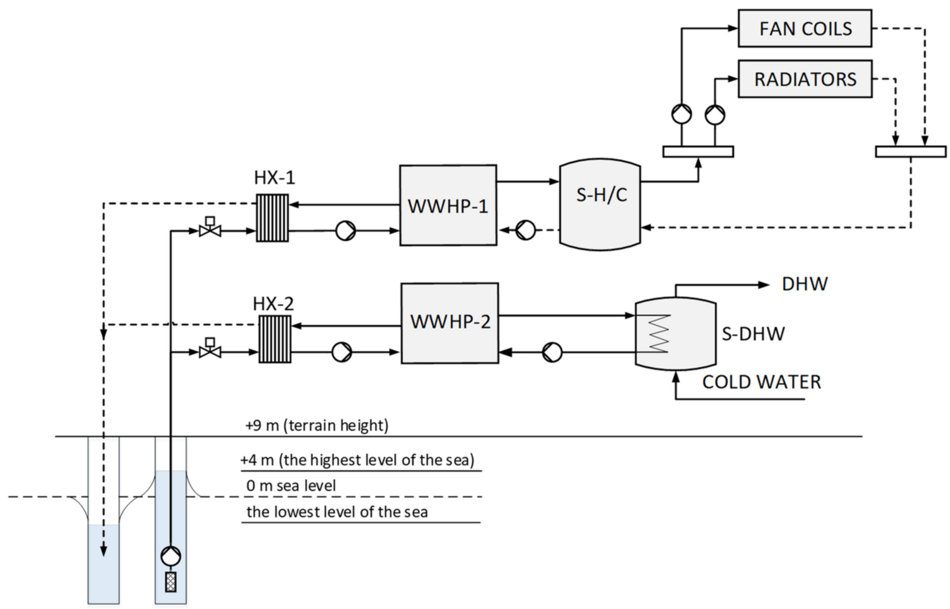

Figure 7. Scheme of HVAC system with WWHP units.

Two subsystems are provided: the subsystem for heating and cooling via heat pump WWHP-1 and the subsystem for heating DHW via heat pump WWHP-2. In heating operation, the heat is transferred to heat pump evaporators, while in the cooling operation the heat from WWHP-1 heat pump condenser is rejected to groundwater. Heat from the groundwater is exchanged between sea water and heat pump loops by heat exchangers HX-1 and HX-2. Each WWHP unit has a separate groundwater HX-1 and HX-2, thus allowing simultaneous operation in different modes: heating or cooling of building by

WWHP-1 or DHW heating by WWHP-2. Design temperature regimes for the equipment in the system are presented in Table 2. Heat pump WWHP-1 is reversible water-to-water heat pump. The unit is sized to cover heating and cooling design capacities at temperature regimes presented in Table 2. The heat pump WWHP-2 is standard type unit sized to cover the heating capacity of 16.5 kW at the condenser outlet water temperature 50 °C and evaporator inlet water temperature of 13 °C.

Table 2. Design temperature regimes for the equipment in WWHP system.

Unit	Operation	Groundwater Temperature Regime	Water Temperature Regime	WWHP Temperature Regime
WWHP-1	Heating	15/11 °C (HX-1)	13/9 °C (evaporator)	40/45 °C (condenser)
WWHP-1	Cooling	19/23 °C (HX-1)	21/25 °C (condenser)	12/7 °C (evaporator)
WWHP-2	Heating	15/11 °C (HX-2)	evaporator: 13/9 °C	45/50 °C (condenser)

WWHP units are simulated using the model Type203 developed by the authors and described in detail in Ref. [30] The model is based on a standard Trnsys WWHP model but is altered with implementation of outlet water set point temperature and variable unit efficiency as a function of system temperatures and partial load efficiency.

Buffer tank is provided in the WWHP-1 heat pump loop towards heat distribution to disable frequent cycling of heat pump. Volume of the tank is 2 m^3. Variable speed pumps are provided for circulation of water in heat source and sink circuits of heat pumps. Heat pump WWHP-1 is provided with two circulation pumps, each with maximal electrical power 750 W. The maximal electrical power of two circulation pumps connected to heat pump HP-1 is 75 W each. The pumps speed is controlled to maintain design temperature difference during operation: 4 K towards heat exchanger HX-1 or HX-2, and 5 K towards the distribution system.

The groundwater pump is a multi-stage submersible pump Grundfos SP 30-3 suitable for pumping of high salinity water. Selected pump can meet the required head operating in the range from 60 to 100% of rotating speed so the frequency control of this pump is provided. The geodetic lifting height of 100 kPa is adopted for supplying groundwater to the WWHP system installation. Performance in variable speed operation is determined from the technical data catalogue for the selected pump. Three different operation regimes are proposed (Table 3). When both WWHP units are operating at the same time, the required flow rate is 6 L/s and the required pressure drop is approximately 180 kPa (regime A). When only the heat pump WWHP-1 is in operation, the flow required is 4.5 L/s and the pressure drop is 160 kPa (regime B), while during the operation of the heat pump WWHP-2 the flow is 1.5 L/s and the pressure drop is 130 kPa (regime C). The proposed operation ensures reduction of electricity consumption as well as the reduction of the total supplied amount of seawater. Overall efficiency presented in Table 3 comprises the efficiency of pump, motor and frequency converter. Control valves are provided to disable the flow of groundwater through an HX whose WWHP is not in operation.

Table 3. Electricity consumption of groundwater pump for different operation regimes.

Regime	WWHP-1	WWHP-2	Flow Rate	Required Pressure Drop	Efficiency	Power Consumption
A	On	On	6 L/s	180 kPa	50.5%	2.137 kW
B	On	Off	4.5 L/s	160 kPa	45.9%	1.568 kW
C	Off	On	1.5 L/s	130 kPa	22.2%	0.879 kW

3.2.2. HVAC System with AWHP

Simple schematic of the system with air-to-water heat pumps is presented in Figure 8. The reversible air-to-water heat pump (AWHP-1) is intended for heating and cooling the building. The unit is sized to cover design heating capacity at 45/40 °C water temperature and an outside air temperature of −6 °C. Design cooling capacity must be supplied at outdoor air temperature of 35 °C and an evaporator water temperature 12/7 °C. For DHW heating (AWHP-2), a standard heat pump unit with a nominal heating output at condenser water temperature of 45/50 °C and an outside air temperature of −6 °C is provided.

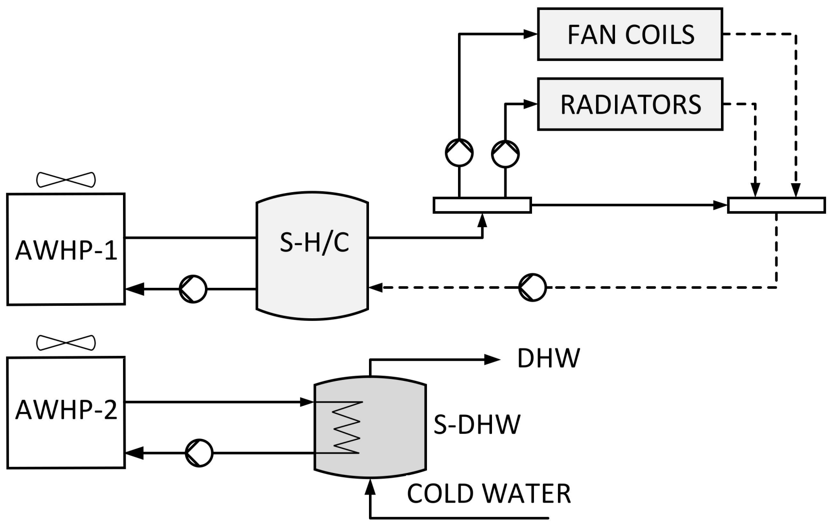

Figure 8. Scheme of HVAC system with AWHP units.

Air-to-water heat pumps can also be installed in the boiler room in the auxiliary building, since the unit fans have sufficient external static pressure. In this case, adequate openings for air supply on the facade should be ensured, as well as the air outlet through short sheet metal ducts.

AWHP units are simulated using the model Type203, developed by the authors and described in Ref. [30] The model is based on the standard Trnsys AWHP model, with implementation of the outlet water set point temperature and variable unit efficiency as a function of system temperatures and partial load efficiency.

Pumps are provided for the circulation of water in heat distribution circuits. Heat pump AWHP-1 has a circulation pump with a peak electrical power of 750 W, while the power of the circulation pump connected to the heat pump is AWHP-2 is 75 W. Both pumps are frequency controlled to ensure 5K temperature difference during operation.

3.2.3. Heat Pump Units

Heat pumps from four European manufacturers were considered (Aermec, Ciat, Daikin, Ecoforest). To avoid the promotion of a manufacturer or product, the manufacturers are labeled with letters from A to D, which are not related to the manufacturer's name. The units are presented in Table 4.

Manufacturer data for performance at partial load were provided only for certain units (AWHP A, AWHP C, WWHP D). The change in partial load factor *PLF* with reduction of heat pump load *PLR* for heating operation is presented in Figure 9. The general trend is the rise of efficiency of heat pump with the reduction of capacity.

Table 4. Investment cost, possibility for capacity control and provided PLF data for heat pump units considered in the analysis.

Manufacturer	Heat Pump Type	Refrigerant	Capacity Modulation	*PLF* Data Provided	Price for 2 Heat Pumps (H/C and DHW)
A	AWHP	R32	Yes (12–100%, stepless)	Yes	55.500 €
B	AWHP	R410A	Yes (50, 100%)	No	34.500 €
C	AWHP	R410A	Yes (25, 50, 75, 100%)	Yes	32.600 €
A	WWHP	R410A	No (on-off)	No	23.800 €
B	WWHP	R410A	Yes (50, 100%)	No	21.700 €
C	WWHP	R410A	No (on-off)	No	13.000 €
D	WWHP	R410A	Yes, (20–100%, stepless)	Yes	37.000 €

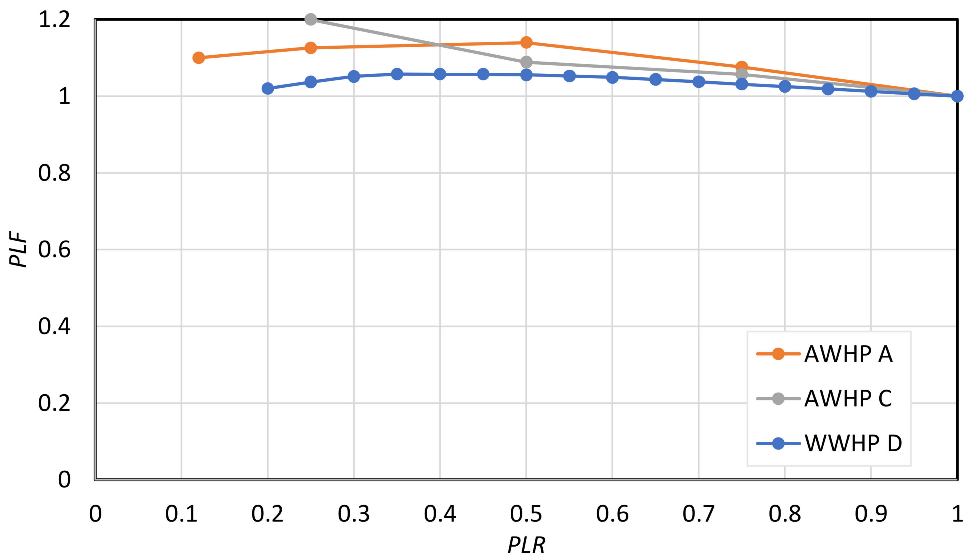

Figure 9. Change of partial load factor *PLF* with partial load ratio *PLR* for operation of heat pump in heating.

3.2.4. PV System

The placement of PV modules produced by Croatian manufacturer, type Solvis SV60 300E on the roof of the auxiliary building is proposed in combination with both of the heat pump systems. The number of modules is determined by the requirement to cover the nonrenewable part of the electricity required to run the H/C and DHW system. Modules are divided on two arrays equally and can in all cases be placed on the roof of auxiliary building. The arrays are oriented towards SE and NW and placed at the inclination of 20°. Each module has total area of 3.25 m^2 which results in 0.6 kW of the nominal power. The panels are monocrystalline with a declared efficiency of 18%. The PV system was simulated using the Trnsys model Type562d. The electricity from PV is used to replace the non-renewable consumption of heating and cooling energy production systems, while the consumption for other systems in the building is not considered (e.g., lighting, fan coils, appliances . . .), so the surplus is considered to be sold to the grid. Given the current conditions for connecting a PV power plant to the grid in Croatia (so-called "net metering"), according to which electricity delivered to the grid is recognized to the prosumer at the same price as purchased if its production is less than or equal to the prosumer's consumption, it follows that it is not necessary to install the accumulation of electricity, because the entire electric power system serves as an accumulation under the stated conditions.

3.3. Costs

EU guidelines [33,34] were applied in the present study for calculation of total cost. The global cost is considered through investment, operating and maintenance cost.

The calculation procedure is repeated for each year of the calculation period, which in this case is adjusted to 15 years as an expected lifetime of heat pump units according to Ref. [35] The real discount rate of 3% is determined with reference to the trend registered for Croatia.

Investment cost includes only the costs of the energy production (heat pump) system and the cost of the PV system. The heat pump system costs include the cost of installation of heating and cooling equipment in the machine room. The costs of EEM on the building envelope and the heat distribution and emission via fan coils are the same for all variants, so they are also omitted in order to achieve a clearer insight into the effect of heat pump choice on cost efficiency. Procurement costs include investments for all major equipment. The cost of installation and associated works was estimated at 20% of the equipment procurement cost. Investment costs are presented in Table 5.

Table 5. Investment costs.

System	Description	Price
WWHP	Groundwater heat source system (mechanical and geotechnical works) Auxiliary HVAC equipment and related installation works	53.000 €
AWHP	Auxiliary HVAC equipment and related installation works	13.000 €
PV	Procurement and construction of PV power plant	800 €/kW

Annual operating costs depend on the price of electric energy and equipment maintenance. Concession for groundwater use is included in energy costs as it mainly depends on water consumption, which varies with energy consumption (Table 6). The fee for the engaged electric power is not charged in the considered tariff model, which is the same as for households and is applied by the user.

Table 6. Energy prices.

Energy Source		Cost	Price
Electricity	Day tariff	0.083	€/kWh
	Night tariff	0.052	€/kWh
Groundwater		0.013	€/m^3

The maintenance cost of HVAC systems is estimated at 3% of the investment price. For the PV system, the maintenance cost is minimal and includes a cleaning of the modules surface once a year (100 €).

4. Results

Results of simulations for AWHP and WWHP systems in the case with neglected *PLF* (S1) is presented in Figure 10. Solutions considering specific global cost and specific electricity consumption from the grid are evaluated according to the Pareto concept.

A cost-optimal solution that minimizes the global cost over the predicted life cycle is the AWHP system with the unit produced by manufacturer C. An energy-optimal solution that minimizes the electric energy consumption is the WWHP system, with the unit by manufacturer B. Th results show that the solutions are grouped regarding the system type: WWHP systems have lower electricity consumption with a higher global cost, while AWHP-based systems have a higher electricity consumption with a lower global cost.

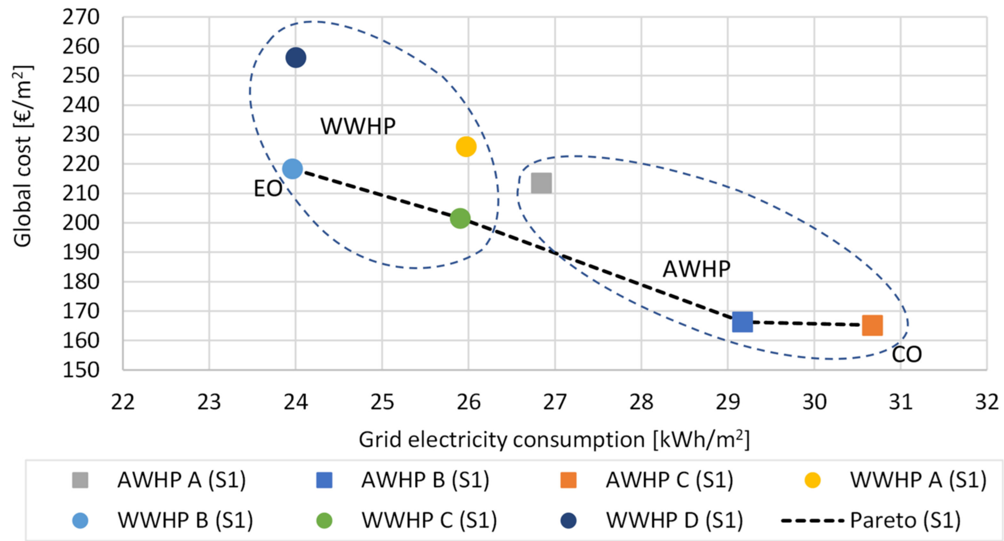

Figure 10. Results of global cost and grid electricity consumption from simulations for AWHP and WWHP systems with PV collectors covering nonrenewable part of electricity for the case with neglected *PLF* (scenario 1).

Additional simulations are conducted for systems with AWHP A and C, and WWHP D unit, for the case when *PLF* data provided from the manufacturer is used (S2). Figure 11 presents these results combined with previous results from S1. The impact of efficiency at partial load is evident for those solutions: S2 solutions have lower costs and lower electricity consumption due to increased efficiency while operating at partial load. A cost-optimal solution is AWHP C, while energy optimal is AWHP A. None of the solutions from the considered WWHP systems are optimal considering energy or cost criterion. Reduced electricity consumption resulting from increased efficiency at a partial load is addressed by indicator X from Equation (7). It ranges from 1.05 (WWHP D), 1.07 (WWHP C) to 1.17 (AWHP A), meaning that the calculated electricity consumption can be up to 17% higher when the unit can operate at a reduced capacity, but the efficiency at the partial load operation is neglected.

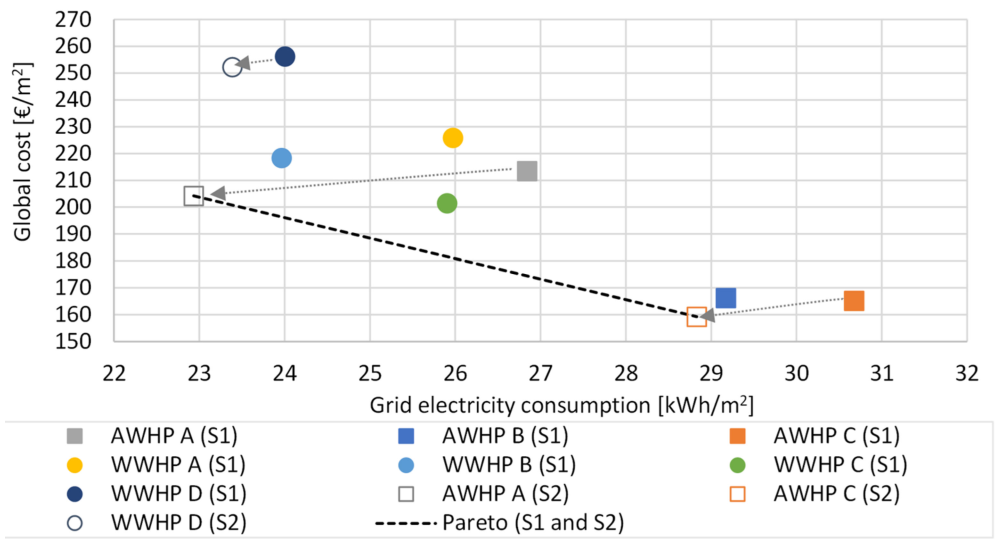

Figure 11. Results of global cost and grid electricity consumption from simulations for AWHP and WWHP systems with PV collectors covering the non-renewable part of the electricity for cases with neglected *PLF* (scenario 1) and the manufacturer-provided *PLF* (scenario 2).

Seasonal efficiencies presented by SCOP and SEER factors for heating, cooling and DHW heating are presented in Figure 12. AWHP system units achieved lower seasonal efficiencies in heating and cooling compared to WWHP systems. Units produced by some manufacturers perform better than those produced by others, meaning that the general conclusion regarding the efficiency of AWHP or WWHP technology cannot be made. Manufacturer A, for example, has almost equally efficient AWHP and WWHP units. The improved efficiency of some units can also be connected to the investment price for the system (Table 7), where the system with the most efficient AWHP unit from manufacturer A has the highest investment cost amongst the AWHP systems. The mentioned also refers to WWHP systems where system WWHP D with the most efficient unit has the highest investment cost.

Cost indicators are presented in Table 7 by global cost, investment cost in the starting year, and operating cost and maintenance cost during the lifetime of system. Despite the lower seasonal efficiency indicated earlier, systems with AWHP units have a lower operating cost compared to WWHP systems. This can be addressed to the greater auxiliary energy required for running pumps in WWHP systems and the cost for pumped ground or sea water. Maintenance costs are a function of investment costs, so the more expensive system will result in a higher maintenance cost and vice versa. The required PV plant array is calculated to cover the non-renewable part of the electricity, which would otherwise be acquired from the grid. The PV plant size applied to HVAC system varies with the energy consumption of the system from 17.4 to 23.4 kW, or is expressed by array size from 94 to 125 m^2.

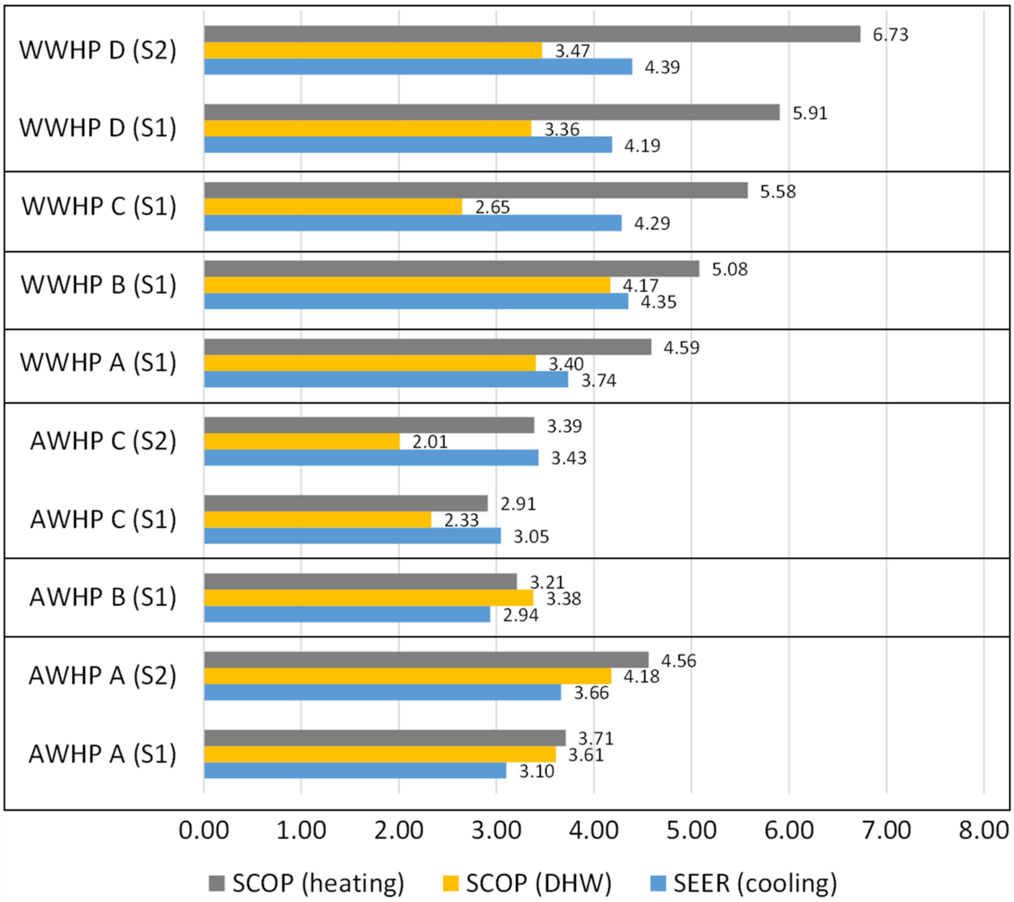

Figure 12. Seasonal efficiency indicators SCOP and SEER for AWHP and WWHP systems, calculated from simulation results for scenarios 1 and 2.

Table 7. Energy, cost and efficiency indicators and PV plant size (PV collectors covering nonrenewable electricity consumption).

System	Electricity from Grid, kWh/m^2	Global Cost, €/m^2	Investment, €/m^2	Operating Cost, €/m^2	Maintenance Cost, €/m^2	PV Plant Size, kW
AWHP A (S1)	27.0	213.5	139.0	27.8	46.7	20.4
AWHP B (S1)	29.2	166.3	103.9	29.9	32.5	21.6
AWHP C (S1)	30.7	165.2	102.7	31.3	31.2	23.4
WWHP A (S1)	26.0	225.9	141.2	37.0	47.8	19.8
WWHP B (S1)	24.0	218.4	136.1	35.9	46.3	18.6
WWHP C (S1)	25.9	201.6	122.4	38.7	40.5	19.8
WWHP D (S1)	24.0	256.2	162.7	36.8	56.7	18.6
AWHP A (S2)	22.9	204.2	135.5	22.0	46.7	17.4
AWHP C (S2)	28.8	159.3	100.6	27.5	31.2	21.6
WWHP D (S2)	23.4	252.4	161.3	34.4	56.7	17.4

Achieved seasonal efficiencies of WWHP and AWHP units for heating and cooling of the building derived from simulation results are compared to those which can be found at the certification website from Ref. [11] (Figure 13). Values from the simulation and certification database do not match and the difference is present. Moreover, the order of efficiency by units established by simulation is not supported by the data from the certification database.

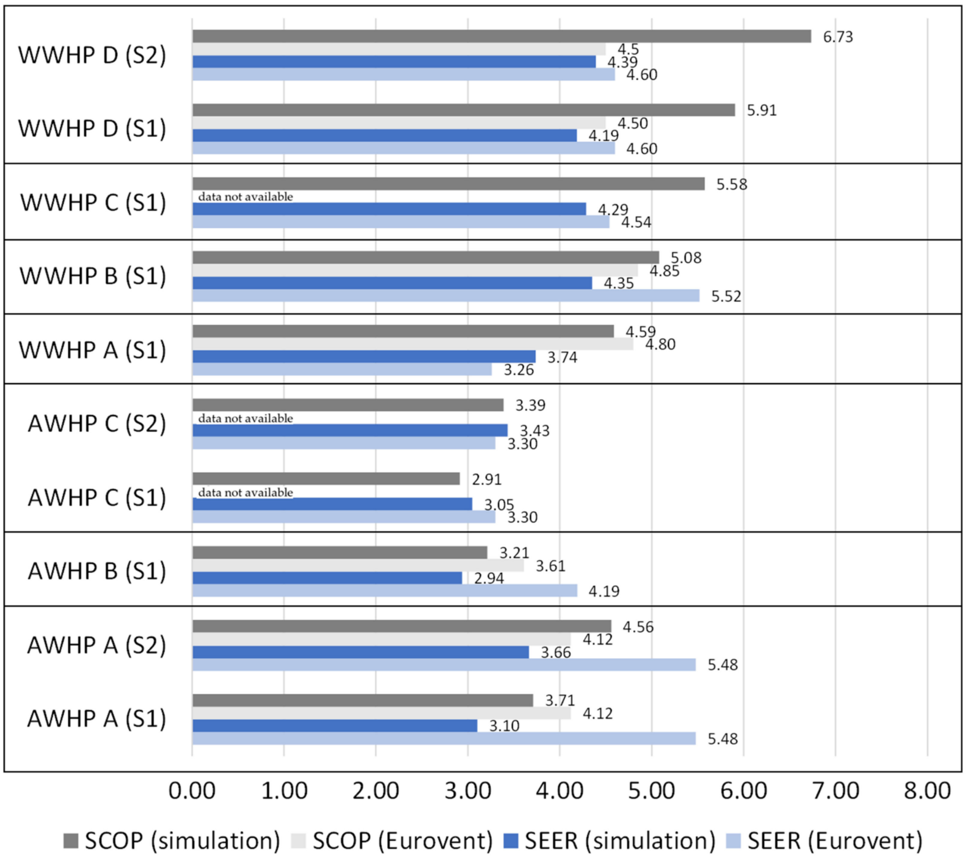

Figure 13. Comparison of seasonal efficiency indicators SCOP and SEER for AWHP and WWHP systems calculated from simulation results to values determined from Ref. [11].

Payback periods are compared for the AWHP C system for scenario S2 in the case of a sole HVAC system without PV and for the cost-optimal system with PV modules (Figure 14). The payback period for the system with PV modules is that approximately 12 years afterwards, it reduces the global cost.

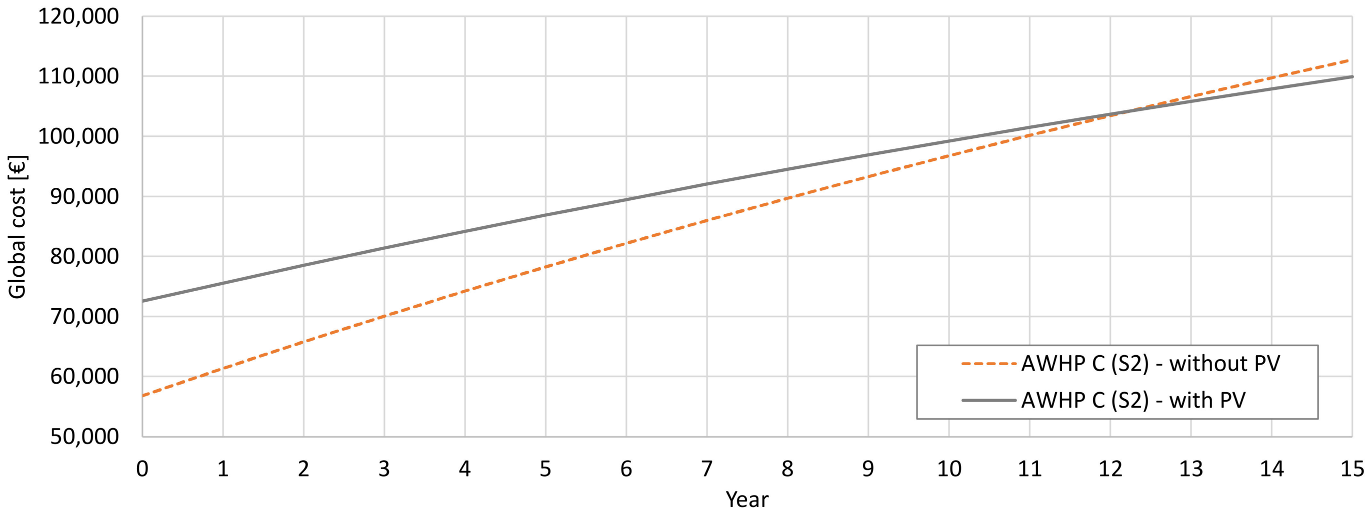

Figure 14. Payback period for cost optimal system AWHP C.

5. Discussion

Insight into Figures 10 and 11 shows that for the considered building, the chosen system and building energy consumption dynamics and system dynamics AWHP heat pumps represent optimal solutions considering lifetime costs. The advantage of AWHP compared to WWHP cannot be concluded generally. For example, AWHP B and AWHP C represent most cost-effective cases, but if the analysis covered AWHP A and WWHP C units only, it could result in a different conclusion and could give advantage to WWHP C. Higher SCOP and SEER, provided by certification organizations, e.g., Ref. [11], does not mean that the system will be cost-effective during the considered lifetime. The influence of investment costs is very important, and it can be noticed that producers of more effective equipment carefully include that advantage into their higher prices. Cases with a higher energy consumption for the building, such a price increases, can pay off, but for lower energy consumption, the application of such heat pumps may not pay off.

Analysis is performed for a life expectation time of 15 years for all the equipment. The problem is that the lifetime can vary between different manufacturers, depending on the quality of implemented components and the action of the control system, and such data are not presented by manufacturers. This makes the results of the analyses questionable. Therefore, more research of the equipment lifetime, such as Ref. [35], would be welcome.

The influence of partial load operation efficiency is visible from Figure 11 for heat pumps produced by manufacturers who publish their part load data AWHP A, AWHP C and WWHP D. For that, heat pumps, electric energy consumption and global costs are decreased for S2 solutions compared with S1 due to the efficiency increase. The problem appears with applications of certification organization data for SCOP and SEER, as those values differ from simulation data (Figure 12) due to the fact that SCOP and SEER values are given for a fixed hypothetic dynamic of consumption, which is not applicable to all cases and climate influences. This fact points out the necessity of the publication of complete operational data for full and partial loads data for the entire temperature application field by manufacturers. Such data can then be suitable for dynamic simulation for different climate data available from meteorological databases, such as Joint Research Centre database [36].

6. Conclusions

The objective of this paper was to determine the cost optimality between HVAC systems using AWHP and WWHP. The analysis is performed for a certain number of fixed and variable capacity heat pump units, from four manufacturers available on the European market. The analysis is performed on the case study of a nursery building located on the Adriatic coast in Poreč (Croatia). The dynamic simulations of building and HVAC systems were performed using the Trnsys software. The results show that the partial load efficiency of the heat pump should not be neglected in the analysis of the application, while the difference in energy consumption and cost can be up to 17%. It is noted that the analysis must be performed for a wider range of units, especially when heat pump systems with different sources are considered. The HVAC system using AWHP units with capacity control is the cost-optimal solution. The application of the photovoltaic (PV) system sized to cover the non-renewable portion of the HVAC system's electricity consumption has a payback period of 12 years.

The considered building is not the typical (referent) educational building of Croatia. The building has the typical architecture of the Austro-Hungarian Empire in Istria at the end of 19th century. It is located in the protected cultural and historical zone of the city. In old town centers in the northern part of the Croatian Adriatic coast, many similar buildings can be found. In the presented case study, the building had a specific purpose, which was characterized by the operating schedules, heating and cooling interruptions, and heat gains. A similar result regarding the HVAC system with heat pumps can be expected for office buildings, but in future studies, additional analysis will be performed to confirm this assumption. Analysis on a residential building can also be interesting and could have an applicative value considering the use of existing buildings of this type in Croatia (from offices and public services to residential).

In the present situation where energy prices rise significantly, inflation accelerates and new refrigeration systems with a low GWP and natural refrigerants appear in the market; the calculations of long-term cost efficiency are rather unreliable and hard to perform. Nevertheless, decisions on system and equipment choice still must be performed and it is important that analyses are comprehensive, keeping in mind all possible situations. In such a situation, energy efficiency and renewable energy source applications are very important topics to consider.

Author Contributions: Conceptualization, B.D. and B.P.; methodology, B.P.; software, B.D. and L.B.; validation, B.D. and B.P.; formal analysis, M.G.; investigation, B.D.; resources, B.P.; data curation, B.P. and B.D.; writing—original draft preparation, B.D., B.P. and L.B.; writing—review and editing, B.D., B.P. and M.G.; visualization, B.D.; supervision, B.P.; project administration, B.P.; funding acquisition, B.P. All authors have read and agreed to the published version of the manuscript.

Funding: This research was funded by University of Rijeka project (uniri-tehnic-18-14).

Institutional Review Board Statement: Not applicable.

Informed Consent Statement: Not applicable.

Data Availability Statement: Not applicable.

Conflicts of Interest: The authors declare no conflict of interest.

Abbreviations

A	area (m^2)
C_g	global cost (€)
CI	cost indicator (€/m^2)
E	energy (kWh)
EI	energy indicator (kWh/m^2)

f	primary energy factor (-)
U	overall heat transfer coefficient (W/m^{2}K)
X	energy ratio (-)
aux	auxiliary
AWHP	air to water heat pump
c	cooling
COP	coefficient of performance
DHW	domestic hot water
EEM	energy efficiency measure
EER	energy efficiency ratio
GWP	global warming potential
h	heating
H/C	heating and cooling
hp	heat pump
HVAC	heating, ventilation and air conditioning
HX	heat exchanger
nren	nonrenewable
PLF	partial load factor
PLR	partial load ratio
PV	photovoltaic
s	system
SCOP	seasonal coefficient of performance
SEER	seasonal energy efficiency ratio
TRY	test referent year
WWHP	water to water heat pump

References

1. Nocera, F.; Giuffrida, S.; Trovato, M.R.; Gagliano, A. Energy and New Economic Approach for Nearly Zero Energy Hotels. *Entropy* **2019**, *21*, 639. [CrossRef] [PubMed]
2. Corrado, V.; Murano, G.; Paduos, S.; Riva, G. On the Refurbishment of the Public Building Stock toward the Nearly Zero-Energy Target: Two Italian Case Studies. *Energy Procedia* **2016**, *101*, 105–112. [CrossRef]
3. Becchio, C.; Corgnati, S.P.; Vio, M.; Crespi, G.; Prendin, L.; Magagnini, M. HVAC solutions for energy retrofitted hotel in Mediterranean area. *Energy Procedia* **2017**, *133*, 145–157. [CrossRef]
4. Smitt, S.; Tolstorebrov, I.; Gullo, P.; Pardiñas, A.; Hafner, A. Energy use and retrofitting potential of heat pumps in cold climate hotels. *J. Clean. Prod.* **2021**, *298*, 126799. [CrossRef]
5. Vujnović, N.; Dović, D. Cost-optimal energy performance calculations of a new nZEB hotel building using dynamic simulations and optimization algorithms. *J. Build. Eng.* **2021**, *39*, 102272. [CrossRef]
6. Belussi, L.; Barozzi, B.; Bellazzi, A.; Danza, L.; Devitofrancesco, A.; Fanciulli, C.; Ghellere, M.; Guazzi, G.; Meroni, I.; Salamone, F.; et al. A review of performance of zero energy buildings and energy efficiency solutions. *J. Build. Eng.* **2019**, *25*, 100772. [CrossRef]
7. Fahlén, P. Capacity control of heat pumps. *REHVA Eur. HVAC J.* **2012**, *49*, 28–31.
8. Uhlmann, M.; Bertsch, S.S. Theoretical and experimental investigation of startup and shutdown behavior of residential heat pumps. *Int. J. Refrig.* **2012**, *35*, 2138–2149. [CrossRef]
9. Waddicor, D.A.; Fuentes, E.; Azar, M.; Salom, J. Partial load efficiency degradation of a water-to-water heat pump under fixed set-point control. *Appl. Therm. Eng.* **2016**, *106*, 275–285. [CrossRef]
10. Riviere, P.; Malaspina, N.F.; Lebreton, J.M. A New Installation for Part Load Testing of Air to Water Single Stage Chillers and Heat Pumps. In Proceedings of the 2004 International Refrigeration and Air Conditioning Conference, West Lafayette, IN, USA, 12–15 July 2004; p. 726.
11. Eurovent Certita Certification. Available online: https://www.eurovent-certification.com/en/ (accessed on 26 January 2022).
12. Schibuola, L.; Scarpa, M. Experimental analysis of the performances of a surface water source heat pump. *Energy Build.* **2016**, *113*, 182–188. [CrossRef]
13. Zacà, I.; D'Agostino, D.; Congedo, P.M.; Baglivo, C. Assessment of cost-optimality and technical solutions in high performance multi-residential buildings in the Mediterranean area. *Energy Build.* **2015**, *102*, 250–265. [CrossRef]
14. Marini, D. Optimization of HVAC systems for distributed generation as a function of different types of heat sources and climatic conditions. *Appl. Energy* **2013**, *102*, 813–826. [CrossRef]
15. Filotico, L.; Piccininni, F.; Scialpi, T. A Taranto's hotel apllication of sea water air heat pump. In Proceedings of the International Conference on Heat Transfer, Thermal Engineering and Environment, Corfu, Greece, 20–22 August 2005.
16. Wang, W.; Zhang, S.; Li, Z.; Sun, Y.; Deng, S.; Wu, X. Determination of the optimal defrosting initiating time point for an ASHP unit based on the minimum loss coefficient in the nominal output heating energy. *Energy* **2020**, *191*, 116505. [CrossRef]

17. Rossi di Schio, E.; Ballerini, V.; Dongellini, M.; Valdiserri, P. Defrosting of Air-Source Heat Pumps: Effect of Real Temperature Data on Seasonal Energy Performance for Different Locations in Italy. *Appl. Sci.* **2021**, *11*, 8003. [CrossRef]
18. *ASHRAE Standard 116-1995*; Method of Testing for Rating Seasonal Efficiency of Unitary Air Conditioners and Heat Pumps. ASHRAE Standard: Atlanta, GA, USA, 1995.
19. *EN 14825:2019*; Air Conditioners, Liquid Chilling Packages and Heat Pumps, with Electrically Driven Compressors, for Space Heating and Cooling—Testing and Rating at Part Load Conditions and Calculation of Seasonal Performance. European Standards: Brussels, Belgium, 2019.
20. *UNI 10963*; Air Conditioners, Liquid Chilling Packages And Heat Pumps—Performance Tests at Part Load. Ente Nazionale Italiano di Unificazione (UNI): Rome, Italy, 2001.
21. *Energy in Croatia—Annual Energy Report 2019*; The Ministry of Economy and Sustainable Development: Zagreb, Croatia, 2020.
22. Eurostat (European Statistical Office). 2022. Available online: https://ec.europa.eu/eurostat (accessed on 26 January 2022).
23. TRNSYS Transient System Simulation Tool. 2013. Available online: http://www.Trnsys.Com/ (accessed on 17 January 2022).
24. Soldo, V.; Novak, S.; Horvat, I. *Algorithm for Calculating the Energy Required for Heating and Cooling Building Space According to HRN EN ISO 13790*; Faculty of Mechanical Engineering and Naval Architecture, University of Zagreb: Zagreb, Croatia, 2017.
25. Recknagel, E.; Sprenger, H.; Schramek, E.-R. *Taschenbuch fur Heizung und Klimatechnik*; Oldenbourg Industrieverlag: Munchen, Germany, 2007.
26. Meteonorm Meteonorm—Global Meteorological Database. Available online: https://www.energiehaus.es/wp-content/uploads/2015/06/flyer-meteonorm-7.pdf (accessed on 10 January 2022).
27. Technical Regulation on Rational Use of Energy and Thermal Protection in Buildings, Croatia. 2015. Available online: https://narodne-novine.nn.hr/clanci/sluzbeni/dodatni/438515.pdf (accessed on 17 January 2022).
28. *EN 12831*; Energy Performance of Buildings—Method for Calculation of the Design Heat Load. European Committee for Standardizations: Brussels, Belgium, 2017.
29. Richtlinie VDI 2078 Blatt 1. Berechnung der Kühllast klimatisierter Gebäude bei Raumkühlung über Raumumschließungsflächen. *Bauphysik* **2003**, *25*, 172–173. [CrossRef]
30. Delač, B. *Optimization of Energy Systems for Nearly Zero Energy Buildings Using Dynamic Simulations*; University of Rijeka—Faculty of Engineering: Rijeka, Croatia, 2017.
31. Pavković, B.; Delač, B.; Mrakovčić, T. Modified water loop heat pump system for a hospital with complex HVAC systems. *Teh. Vjesn. Gaz.* **2012**, *19*, 621–631.
32. Pavković, B.; Jelušić, K.; Frank, M. Optimization of the Heat Pump Systems Using Surface Water at Low Temperatures as the Heat Source. In Proceedings of the 38th International Congress on Heating, Ventilation and Air-Conditioning, SMEITS, Belgrade, Serbia, 5–7 December 2007; SMEITS: Belgrade, Serbia, 2007; pp. 253–264.
33. Commission Delegated Regulation No. 244/2012. 2012. Available online: http://www.buildup.eu/sites/default/files/content/l_08120120321en00180036.pdf (accessed on 17 January 2022).
34. European Union. *Guidelines Accompanying Commission Delegated Regulation (EU) No 244/2012 of 16 January 2012 Supplementing Directive 2010/31/EU of the European Parliament and of the Council (2012/C 115/01)*; European Union: Brussels, Belgium, 2012.
35. ASHRAE: Service Life and Maintenance Cost Database. Available online: http://weblegacy.ashrae.org/publicdatabase/ (accessed on 26 January 2022).
36. Joint Research Centre—Photovoltaic Geographical Information System. Available online: https://re.jrc.ec.europa.eu/pvg_tools/en/ (accessed on 26 January 2022).